Pergamon

0960-1481(94)E0021-V

Renewable Energy, Vol. 6, No. 2, pp. 129–138, 1995

0960-1481/95 $9.50+0.00

REVIEW AND TEST OF METHODS FOR DETERMINATION OF THE SOLAR CELL SERIES RESISTANCE

M. BASHAHU and A. HABYARIMANA

Department of Physics, Faculty of Sciences, National University of Rwanda, P.O. Box 117 Butare, Rwanda

(*Received* 3 *February* 1994; *accepted* 12 *April* 1994)

Abstract—About 20 methods of determining the solar cell series resistance R_s are reviewed. Their differences lie principally in: (i) experimental conditions (darkness or illumination, flash or constant illumination, static or dynamic mode, temperature conditions, frequential or non-frequential regime); (ii) number of diodes quoted in the solar cell model; (iii) other assumptions (constant ideality factor or not, infinite or finite shunt resistance); (iv) simultaneous determination of other parameters or not. Before discussing their specifications, the authors assess 12 of them using a commercial single-crystal silicon solar cell (78.5 cm^2 total area).

The obtained R_s values extend from 0.4 to 55.1 $m\Omega\ cm^{-2}$. Those values are compared to results from other workers which lie in the following interval: [0; 1600] $m\Omega\ cm^{-2}$. Those discrepancies are due essentially to: (i) intrinsic differences amongst the methods; and (ii) differences in solar cell basic materials, structures, fabrication modes and areas. This second kind of discrepancy is found to be the principal reason of discordance between our results and those of other workers. Furthermore, one can note that R_s values decrease when solar cell area increases. This is in agreement with the Lindmayer and Allison relationship between R_s and the number of front ohmic contact fingers.

1. INTRODUCTION

Solar cell principal electrical parameters such as short-circuit current density J_{sc}, open-circuit voltage V_{oc}, maximum power P_m, fill factor FF and maximum conversion efficiency η_m are decreasing functions of solar cell series resistance R_s as illustrated [1] in Fig. 1(a). So, during a solar cell's conception and process, one may search for how to cancel or at least minimize all the factors which increase R_s. This isn't possible if we can't determine this parameter. As a matter of fact, relevant literature proposes various techniques to derive R_s. In this paper, we briefly describe the most important of those methods and we assess experimentally some of them. A synthetic table of the quoted methods is given, together with comments on results, operating conditions and assumptions.

Experiments are performed on a blue commercial single-crystal silicon solar cell (total area 78.5 cm^2; active area 75.1 cm^2) and, as shown in Fig. 1(b–f), simple arrangements are used to carry out I–V measurements under either darkness and illumination conditions or static and dynamic modes. Having encapsulated our cell in a glassy material [Fig. 1(c)], its temperature is assumed to be the mean value between the two values measured with iron/constantan thermocouples on the front and rear faces of the cell's cover, respectively. In Fig. 1(e), different illumination levels are obtained by varying the solar cell's distance from the solar simulator.

Furthermore, in order to limit the solar cell's heating by the solar simulator, we have placed between the latter and the former a sheet of compact papyrus onto which an aluminium reflecting thin film has been set down and in which an aperture, just large enough to admit light from the simulator to the solar cell and its close vicinity, has been cut. Excessive heating of the solar cell is also avoided by depositing it in an ice bath. In this way, within the short duration (1–2 min) needed to obtain a complete solar cell's I–V characteristic, its temperature is observed to be almost constant.

2. TESTS IN DARKNESS

2.1. *A static method*

One of the simplest methods starts from the solar cell general operating equation (1),

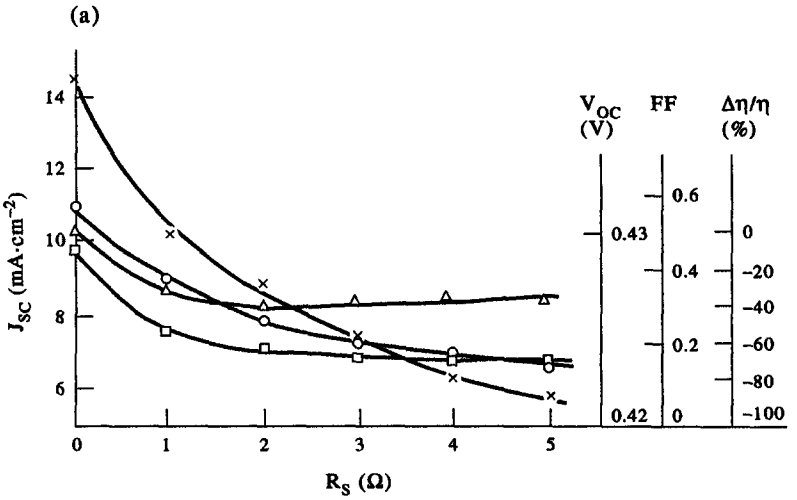

Fig. 1. (a) Variations of $J_{sc}(\times)$, $V_{oc}(\bigcirc)$, $FF(\triangle)$, and $\Delta\eta/\eta(\square)$ with R_s for a p-Si solar cell, area = 12.6 cm^2, under 430 W m^{-2} of illumination, and $T = 300$K. (b) Experimental arrangement for I–V measurements under darkness conditions. C = solar cell; V and V_1 = voltages measured across the solar cell and the resistance R, respectively, with two Keithley digital multimeters; $I = V_1/R$ ($R \approx 1\Omega$; a micro-ammeter is used in reverse bias conditions); Rh = Philip Harris rheostat; E_0 = d.c. emf from a Dynascan tri-output power supply. (c) Solar cell's aspect: c = solar cell; 1 = glassy encapsulation; 2 = front ohmic contact; 3 = rear ohmic contact. (d) Set-up for I–V measurements in dynamic regime under darkness conditions. e = a very low amplitude a.c. signal from a Leader audio generator (visualized on a Leader dual-trace oscilloscope). (e) Experimental set-up for I–V measurements under illumination. R_1 = a Pierron decade resistor box; SS = a 5 kW solar simulator (power supply: 380V; 20A). (f) Arrangement for voltage measurements under flash lamp illumination. V_L and V_{oc} = voltages accross the load resistance R_L and open-circuit voltage respectively; F = intense flash light from the 5 kW solar simulator or from a stroboscope.
(*Continued opposite.*)

$$I = -I_{ph} + \sum_{i=1}^{N} I_{si}\left\{\exp\left[\frac{q}{n_i KT}(V - IR_s)\right] - 1\right\} + \frac{V - IR_s}{R_{sh}}, \quad (1)$$

and makes the following assumptions: (i) one-diode model ($N = 1$; $n_i = n \neq 1$); (ii) darkness operating conditions ($I_{ph} = 0$); (iii) infinite shunt resistance ($R_{sh} \to \infty$) and (iv) high forward bias ($V \nearrow$). Then, eq. (1) is well approximated by relation (2):

$$I = I_s \exp\left[\frac{q(V - IR_s)}{nKT}\right]. \quad (2)$$

Plotting the experimental ln I vs V characteristic in darkness conditions, one can therefore deduce the solar cell R_s value from the gap, on the V-axis, between the actual curve and the diffusion line [2]. Figure 2 summarizes our data at 295K (forward bias and darkness conditions). The resulting R_s value is $(0.093 \pm 0.002)\ \Omega$ for our solar cell, that means $R_s = 1.2$ mΩ cm^{-2}.

2.2. *A dynamic method*

Using solar cell darkness operating conditions, one of the existing dynamic techniques consists of superposing a very low amplitude a.c. signal to a forward electric injection. Then, considering the one-diode solar cell model in which the R_{sh} effects are neglected but not the generation–recombination effects, it takes advantage of eq. (3),

$$I = I_s\left\{\exp\left[\frac{q(V - IR_s)}{nKT}\right] - 1\right\}, \quad (3)$$

to show [3] that a small dynamic variation near a static imposed forward bias ($I = cte$) leads us to eq. (4) for the differential resistance r_d:

$$r_d = \left.\frac{dV}{dI}\right|_{I = cte} = \frac{nKT}{q} \cdot \frac{1}{I} + R_s. \quad (4)$$

Therefore, the solar cell R_s value is obtained by simply reading the intercept value of the $r_d = f(1/I)$ experimental curve with the r_d axis. Figure 3 represents exactly such a curve for our measurements at 301K.

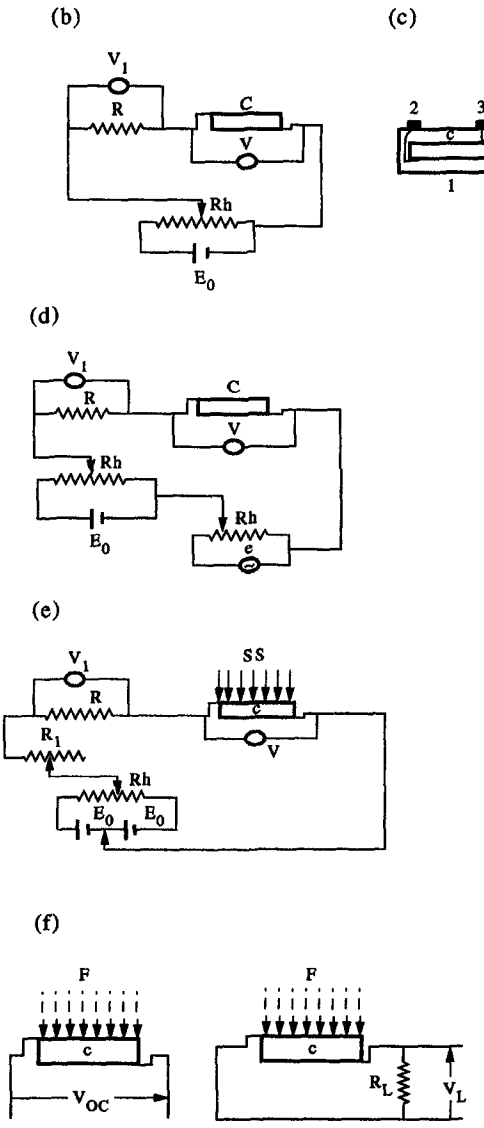

Fig. 1. *Continued.*

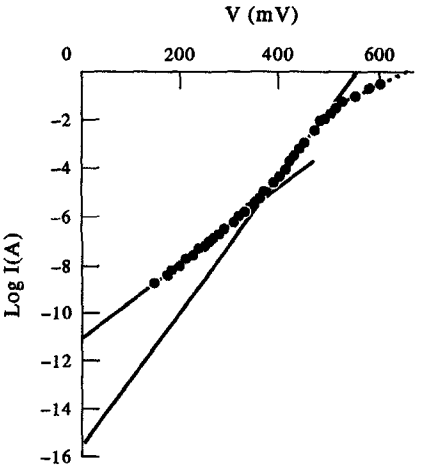

Fig. 2. Dark I–V curve for a c-Si solar cell, area = 78.5 cm^2, T = 295K.

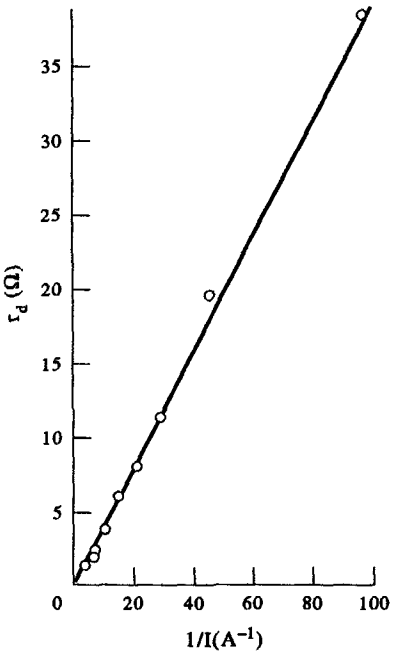

Fig. 3. Dark dynamic resistance curve vs reciprocal current for the same solar cell.

The R_s value deduced from these data is (0.10 ± 0.01) Ω, that is $R_s = 1.3$ mΩ cm^{-2}. A good agreement is noticed between these two first methods.

3. TESTS UNDER ILLUMINATION

3.1. *Method of the slope at the* (V_{oc}, 0) *point*

Utilizing a constant illumination level for the solar cell under investigation and considering the one-diode model in which R_{sh} effects are neglected, one other method derives expression (5) using the slope of one I–V curve at the (V_{oc}, 0) point:

$$R_s = \left.\frac{dV}{dI}\right|_{I=0} - \frac{nKT}{q} \cdot \frac{1}{I_{ph} + I_s}. \tag{5}$$

Using this expression, Fig. 3 and the following data:

$E = 300\ \text{W m}^{-2}$; $T = 321\text{K}$;

$$\left.\frac{dV}{dI}\right|_{I=0} = 0.341\,\Omega; \quad I_{ph} = 0.275\,\text{A};$$

$$n = 1.41; \quad I_s = 1.86.10^{-7}\text{A},$$

we obtain for our solar cell $R_s = (0.30 \pm 0.24)\ \Omega$, that is $R_s = 3.8\ \text{m}\Omega\ \text{cm}^{-2}$.

3.2. *The two characteristics method*

One technique suggested by Swanson in ref. [5] starts from I–V solar cell characteristics under two different illumination levels E_1 and E_2 at the same temperature and derives eq. (6) for R_s:

$$R_s = \frac{\Delta V}{\Delta I_{ph}}. \tag{6}$$

Here, ΔI_{ph} is the difference between the two photogenerated currents I_{ph_2} and I_{ph_1} under illumination levels E_2 and E_1, respectively. ΔV is the difference between the two voltages corresponding to points A_2 and A_1. As indicated in Fig. 4, which summarizes our results under $E_1 = 240\ \text{W m}^{-2}$ and $E_2 = 340\ \text{W m}^{-2}$ at 303K, the two points A_2 and A_1 adjoin the knees of the two curves, and their projections A_2' and A_1' on the I-axis are at the same distance ΔI from I_{ph_2} and I_{ph_1}, respectively.

The R_s value deduced from those results is $(0.36 \pm 0.01)\ \Omega$, that means $R_s = 4.6\ \text{m}\Omega\ \text{cm}^{-2}$. This method is more accurate than the previous one.

3.3. *A flash lamp method*

Based on the one-diode model in which the R_{sh} effects are neglected, one technique [6] derives R_s from measurements of the open-circuit voltage V_{oc} and the voltage V_L across a load resistance R_L when the solar cell is illuminated by one flash from a high intensity flash lamp. Equation (7) is then used:

$$R_s = R_L\left(\frac{V_{oc}}{V_L} - 1\right). \tag{7}$$

Many tests on our solar cell with $R_L = 1.4\ \Omega$ and flashes from a 5 kW solar simulator have given the following mean values:

$$V_L = 116.7\,\text{mV}; \quad V_{oc} = 477.1\,\text{mV}$$

and

$$R_s = (4.3 \pm 2.8)\,\Omega,$$

that is $55\ \text{m}\Omega\ \text{cm}^{-2}$.

3.4. *Method of Quanxi Jia and Anderson*

This method [7], based on the one-diode model, supposes the ideality factor n variable along the I–V characteristic of the solar cell under illumination and derives expression (8) for R_s considering an infinite R_{sh} value:

$$R_s = \frac{V_m}{I_m} \cdot \frac{\frac{1}{V_t}\cdot(I_{sc}-I_m)\left[V_{oc} + V_t \ln\left(1-\frac{I_m}{I_{sc}}\right)\right] - I_m}{\frac{1}{V_t}\cdot(I_{sc}-I_m)\left[V_{oc} + V_t \ln\left(1-\frac{I_m}{I_{sc}}\right)\right] + I_m}. \tag{8}$$

It also derives expression (9) for an n mean value:

$$n V_t = (V_m + I_m R_s)/\ln\left[\left(1-\frac{I_m}{I_{sc}}\right) \cdot \exp\left(\frac{V_{oc}}{I_{sc}}\right) + \frac{I_m R_s}{2V_t} + \frac{I_m}{I_{sc}}\right]. \tag{9}$$

From these expressions, using the following experimental data: $T = 321\text{K}$; $E = 300\ \text{W m}^{-2}$; $I_m = 0.226\ \text{A}$; $V_m = 0.300\ \text{V}$; $I_{sc} = 0.275\ \text{A}$; $V_{oc} = 0.405\ \text{V}$; we find $R_s = (1.32 \pm 0.01)\ \Omega$, that is $R_s = 17\ \text{m}\Omega\ \text{cm}^{-2}$, and $n = 1.48$.

3.5 *Method of Singal*

This technique is also based on the one-diode model and neglects the R_{sh} effects. Like the author [8], one derives analytical expressions of V_m, I_m, P_m and FF vs T, V_{oc}, I_L (photogenerated current) and n for $R_s = 0$ and $R_s \neq 0$, respectively. Next, variations of normalized quantities for V_m, I_m, P_m and FF are expressed in terms of T, V_{oc}, I_L and R_s. Then, variations of two amongst the four normalized quantities, i.e $\Delta(V_m/V_{oc})$ and $\Delta(FF)$, are chosen to determine R_s and

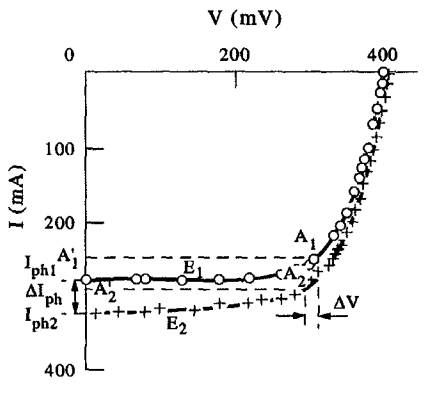

Fig. 4. Light I–V curves for the same cell. $E_1 = 240\ \text{W m}^{-2}$; $E_2 = 340\ \text{W m}^{-2}$; $T = 303\text{K}$.

n using experimental data for the solar cell under one illumination level.

Here are the starting experimental data:

$$E = 300\ \mathrm{W\,m^{-2}};\quad T = 321\mathrm{K};\quad V_{oc} = 0.405\ \mathrm{V};$$

$$I_L = 0.275\ \mathrm{A};\quad \left(\frac{V_m}{V_{oc}}\right)_{R_s \neq 0} = 0.741;$$

$$\left(\frac{V_m}{V_{oc}}\right)_{\substack{R_s \neq 0 \\ n=1}} = 0.824;\quad \left(\frac{V_m}{V_{oc}}\right)_{\substack{R_s = 0 \\ n=2}} = 0.746;$$

$$(FF)_{R_s \neq 0} = +0.610;\quad (FF)_{n=1}^{R_s=0} = 0.759;$$

$$(FF)_{n=2}^{R_s=0} = 0.626.$$

Starting R_s values deduced from $\Delta(FF)$ and $\Delta(V_m/V_{oc})$ are the following:

For $n = 1$,

$$R_s = 0.258\,\Omega \quad \text{from } \Delta(FF) \text{ value},$$

$$R_s = 0.822\,\Omega \quad \text{from } \Delta\left(\frac{V_m}{V_{oc}}\right) \text{value}.$$

For $n = 2$,

$$R_s = 0.221\,\Omega \quad \text{from } \Delta(FF) \text{ value},$$

$$R_s = 0.415\,\Omega \quad \text{from } \Delta\left(\frac{V_m}{V_{oc}}\right) \text{value}.$$

The following step then consists of finding the value of n such that the two R_s results obtained from $\Delta(FF)$ and $\Delta(V_m/V_{oc})$ values converge towards the same quantity.

The $(n,\ R_s)$ couple obtained in this way is $n = 1.40$ and $R_s = (0.10 \pm 0.01)\,\Omega$, that means $R_s = 1.3\ \mathrm{m\Omega\,cm^{-2}}$.

3.6. *Maximum power point method*

Suggested by Picciano (ref. 4 in [9]), this method uses the I–V solar cell characteristic under one illumination level with the assumptions of the one-diode model, an infinite R_{sh} value and a constant n value along the whole characteristic. It derives expressions (10) and (11) for R_s:

$$R_s = \frac{V_m}{I_m} - \frac{1}{B(I_L - I_m)} \tag{10}$$

where

$$B = \frac{[I_m/(I_L - I_m)] + \ln[(I_L - I_m)/I_L]}{2V_m - V_{oc}} \tag{11}$$

with $I_L \simeq I_{sc}$.

Derived from these relationships, the most realistic R_s value resulting from many tests on our solar cell is $R_s = (0.055 \pm 0.024)\,\Omega$, that means $R_s = 0.7\ \mathrm{m\Omega\,cm^{-2}}$.

3.7. *Area method*

Calling A the area between the I–V characteristic under one illumination level and the I and V axes, supposing the one-diode model, an infinite R_{sh} value and a constant n value, this technique (ref. 7 in [9]) shows that R_s can be derived from expression (12):

$$R_s = 2\left(\frac{V_{oc}}{I_{sc}} - \frac{A}{I_{sc}^2} - \frac{nKT}{qI_{sc}}\right). \tag{12}$$

Many tests on our solar cell have led us to the following most realistic R_s value: $R_s = (0.030 \pm 0.016)\,\Omega$, that is $R_s = 0.4\ \mathrm{m\Omega\,cm^{-2}}$.

The accuracy of this technique and of the previous one is so low that negative R_s values are sometimes noticed.

3.8. *Generalized area method*

By making a suitable change of coordinates, one [10] can put the general analytical expression (1) for the solar cell I–V characteristic in an explicit form. After this, in the particular case of the one-diode model where the R_{sh} effects are not neglected, it is shown that one can derive R_s, R_{sh} and n, first by plotting the solar cell characteristic under three different illumination levels E_i $(i = 1\text{–}3)$ at the same temperature T, then by determining the areas A_i between each I–V cuve and the two axes, and finally by solving the three equations linear system (13) where the unknown quantities are r, n and g:

$$\rho_i = \left(\frac{I_{sc}}{2V_{oc}}\right)_i r + \left(\frac{1}{V_{oc}}\right)_i \gamma n + \left(\frac{V_{oc}}{2I_{sc}}\right)_i g - \left(\frac{1}{I_{sc}}\right)_i \gamma g n \tag{13}$$

where

$$\rho_i = \left(\frac{I_{sc}V_{oc} - A}{I_{sc}V_{oc}}\right)_i;\quad r = R_s;\quad \gamma = \frac{KT}{q}$$

and $$g = \frac{1}{R_{sh}}.$$

The following data have been obtained for our solar cell at 321K:

$$E_1 = 240\ \mathrm{W\,m^{-2}};\quad I_{sc_1} = 0.324\ \mathrm{A};$$

$$V_{oc_1} = 0.410\ \mathrm{V};\quad A_1 = 0.1221\ \mathrm{W}$$

$$E_2 = 260\ \mathrm{W\,m^{-2}};\quad I_{sc_2} = 0.336\ \mathrm{A};$$

$$V_{oc_2} = 0.402\,\text{V}; \quad A_2 = 0.1234\,\text{W}$$

$$E_3 = 340\,\text{W m}^{-2}; \quad I_{sc_3} = 0.279\,\text{A};$$

$$V_{oc_3} = 0.403\,\text{V}; \quad A_3 = 0.1083\,\text{W}.$$

The resulting value for R_s is $(0.83 \pm 0.39)\ \Omega$, that is $R_s = 10.6\ \text{m}\Omega\ \text{cm}^{-2}$.

3.9. *Method of the difference between the photogenerated and the short-circuit currents*

Using the one-diode model with neglected R_{sh} effects, this method shows that [11], for high injection levels, the short-circuit current I_{sc} is not a linear function of the illumination level E and that R_s can be derived from expression (14):

$$\ln\left(\frac{I_L - I_{sc}}{I_s}\right) = \frac{q I_{sc} R_s}{n K T}. \tag{14}$$

As a matter of fact, the experimental I_{sc} curve vs E (Fig. 5) is linear for low illumination levels ($E < 750\ \text{W m}^{-2}$) where I_{sc} is equal to the photogenerated current I_L. For higher light intensities, the difference $I_L - I_{sc}$ becomes significantly positive. R_s can be therefore derived from the slope of the experimental ln $(I_l - I_{sc})$ line vs I_{sc} (Fig. 6).

By this method, we obtain $R_s = (0.29 \pm 0.02)\ \Omega$ for our solar cell, that means $R_s = 3.7\ \text{m}\Omega\ \text{cm}^{-2}$.

3.10. *Method of the two-diode solar cell model*

Making the assumption of the two-diode model for a solar cell and taking into consideration the R_{sh} effects, this technique [12] shows that R_s may be derived from eq. (15):

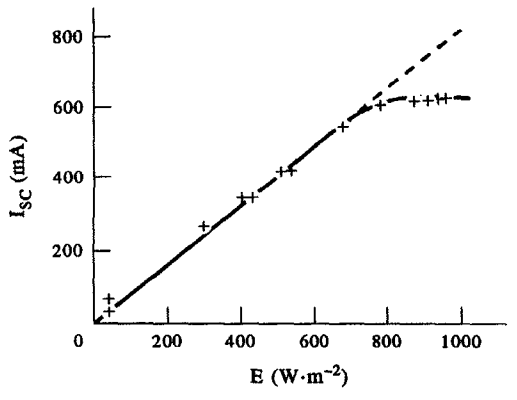

Fig. 5. Short-circuit current/light intensity curve for the same solar cell at 328K.

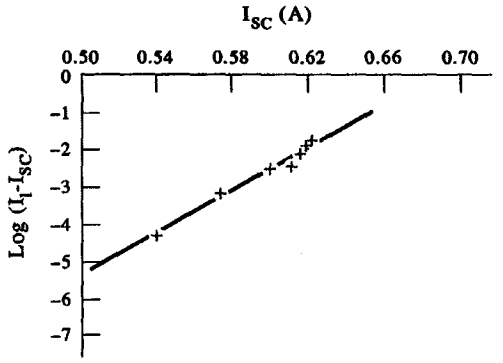

Fig. 6. Variations of $\log(I_l - I_{sc})$ vs I_{sc} for the same solar cell.

$$R_s = -\left[\left(\frac{\partial I}{\partial V}\right)_{V=V_{oc}}\right]^{-1} - \left(\frac{\gamma}{n} I_L\right)^{-1} \tag{15}$$

where $\gamma = q/KT$.

Using this equation and the solar cell characteristic under one illumination level, we find two values for R_s corresponding to $n = 1$ (ideal diode) and $n = 2$ (second-diode factor), respectively. The mean value of these two quantities is a good approximation for the actual R_s value. In this way, we obtain $R_s = (0.190 \pm 0.012)\ \Omega$, that is $2.4\ \text{m}\Omega\ \text{cm}^{-2}$.

One should remark that this method is basically similar to the method of the slope at the $(V_{oc}, 0)$ point, the differences between them consisting of: (i) different numbers of diodes supposed in the models; (ii) neglecting or not the reverse saturation currents; (iii) computing algorithms stated or not in the two methods.

4. OTHER METHODS

In addition to the 12 techniques tested and described above, there exist other methods amongst which we can mention the following:

- a dynamic method [3] in which a low intensity flash with a constant frequency is superposed on a constant light intensity;
- a third dynamic technique [3] where an a.c. signal of very low amplitude with variable frequency is superposed on a constant d.c. forward bias under darkness conditions;
- a method similar to that of Section 3.3, where two different load resistances and two flashes from a high-intensity lamp flash are used [6];
- a technique using one I–V characteristic under illumination and the one-diode model for a simul-

taneous determination of R_s, R_{sh}, I_s and I_{ph} [13];
- one which considers separately the linear and exponential parts of the solar cell I–V dark characteristic in the one-diode model in order to compute R_s, R_{sh}, n and I_s [14];
- two methods, one utilizing the open-circuit voltage decay (OVCD) after a flash illumination [15], another combining light and dark measurements [16], more exactly measure V_{oc} and I_{sc} at different light levels on the one hand, determining the dark forward voltage corresponding to each I_{sc} value on the other hand;
- one method making use of the dark I–V characteristic and the two-diode model to derive simultaneously R_s, R_{sh} and the two reverse saturation current densities J_{01} and J_{02}, thanks to least-square computation techniques [17];
- another one in which I_{sc} and V_{oc} measurements are performed at different light levels and where dark currents corresponding to each V_{oc} value are determined in order to compute the R_s value for a solar cell operating in darkness conditions [18];
- the theoretical one in which R_s is expressed in terms of a solar cell's ohmic front contact's geometric parameters on the one hand, and in terms of the base and emitter conductivities on the other hand [19].

5. COMMENTS

5.1. *On the assumptions and efficiency of the different methods*

As summarized in Table 1, about 20 methods for solar cell series resistance measurement have been presented and some of them have been tested on a commercial single-crystal silicon solar cell. One should remark that most of them utilize static and non-frequential illumination conditions, the one-diode solar cell model, a constant diode factor and an infinite shunt resistance. Another important fact to point out is the assumption of a constant R_s value for any temperature or illumination level considered in all of these methods for a given solar cell. This assumption is unfortunately slightly in discordance with experiment as quoted in different works [6, 18, 20, 21].

Furthermore, the following points should be considered in comparing efficiencies of the different methods presented in this paper.

(i) Methods that use the minimum number of simplifying assumptions from eq. (1) are expected to give the most realistic values for the parameters under investigation, R_s being one of them. Actually, in the one-diode model, physical phenomena are considered globally, so that parameters (which are related to these phenomena) lose their meaning.

(ii) The other conditions remaining the same, techniques making use of chopped light are preferred to those utilizing constant illumination. Effectively, in the former type, one minimizes not only the temperature variation effects on R_s, but also the possible solar cell degradation under extended intense illumination.

(iii) Methods using outdoor-like temperatures and light intensities should be more realistic than those using darkness and/or low temperature conditions. It is actually in the former types of conditions that not only are solar cells expected to operate, but also the physical importance of R_s seems to be obvious.

(iv) Finally, frequential methods (actually rare in literature) are held to be better than non-frequential ones [3].

From these points of view, an absolute classification of the presented methods owing to their efficiency seems to be unthinkable. We should rather give our opinion about the accuracy of results presented in Table 1 and express general comments on them.

5.2. *On the results of the presented methods*

Methods described in Sections 2.1, 2.2, 3.2, 3.4, 3.5, 3.9 and in refs [6, 13–18] are among the most accurate: R_s values obtained from them present less than 10% of relative uncertainty. Contrary to these, techniques which take the computation of slope at the $(V_{oc}, 0)$ point, the maximum power point coordinates, the area between the I–V curve and the two axes, and the resolution of systems of many linear equations, present higher values of relative uncertainty and produce sometimes negative R_s values.

Furthermore, in comparative analysis of the results quoted in Table 1, we should point out the following facts.

(i) Assessment of 12 different methods performed between 295 and 328K (realistic *in situ* temperature conditions) on a commercial single-crystal silicon solar cell (blue, total area 78.5 cm^2, active area 75.1 cm^2) has given R_s values between 0.4 and 55.1 $m\Omega$ cm^{-2}. This interval could be narrowed to [1.2; 16.8] $m\Omega$ cm^{-2} if we had excluded the quite dubious results from the fifth, eighth, ninth and tenth methods in Table 1. Reasons for excluding these have been given in the first paragraph of this section.

Moreover, the high uncertainty in results of the fifth method could come from the following dubious experimental conditions: badly defined flash lifetime;

Table 1. Summary of results, experimental conditions and assumptions stated in various methods for determination of the solar cell series resistance

Method type	Results of this work; Si, single crystal; 78.5 cm^2		Results from other works			
	R_s (mΩ cm^{-2})	T (K)	Ref.	R_s (mΩ cm^{-2})	T (K)	Kind of cell**
1. Static method	1.2±0.0	295±1	[1]	0	298	S-C Si
2. Dynamic method 1	3.2±0.1	301±1	[3]	17.5	299	S-C Si
3. Method of the slope at (V_{oc}, 0)	5.8±2.1	321±2	[6]	6±1*	—	S-C Si, conc.
4. Two characteristics method	4.6±0.0	304±2	[21]	0.2–0.3	295	S-C Si, N/P, 23 cm^2
5. Flash lamp method 1	55.1±22.0	307±2	[6]	6.9±0.2*	—	S-C Si, conc.
6. Quanzi's method	16.8±0.1	321±2	[7]	1600	298	S-C Si, N$^+$/P, 2 cm^2
7. Singal's method	1.3±0.0	321±2	[8]	600*	—	—
8. Maximum power point method	0.7±0.3	307±2	[9]	[−4.3; 9.1]	295	S-C Si, N/P; 23 cm^2
9. Area method	0.4±0.2	302±2	[9]	[−0.2; 0.46]	295	S-C Si, N/P, 23 cm^2
10. Generalized area method	10.6±5.0	306±2	[10]	—	—	—
11. Difference $I_L - I_{cc}$ method	3.7±0.1	328±2	[11]	95	—	S-C Si, N$^+$/P, 4 cm^2
12. Two diode method	2.4±0.2	321±2	[12]	[36.3; 49.5]	—	S-C Si, 4 cm^2
13. Dynamic method 2	—	—	[3]	75*	—	Cu_xS/Cd S
14. Flash lamp method 2	—	—	[6]	7.3±0.8*	—	S-C Si, conc.
15. Charles *et al.*'s method	—	—	[13]	17.4	300	S-C Si, 25.8 cm^2
16. Laplaze and Youm's method	—	—	[14]	[216; 748]	300	S-C Si and text. Si
17. OCVD method	—	—	[15]	1153*	—	S-C Si, N$^+$/P
18. Bhattacharya *et al.*'s method	—	—	[16]; [19]	1286*	—	S-C Si, N$^+$/P
19. Araujo *et al.*'s method	—	—	[17]	10.6; 17.5	300	Si P$^+$/N/$^+$; Si N$^-$/P/P$^+$
20. Imamura and Portocheller's method	—	—	[9]; [18]	0.21; 0.28	295	S-C Si, N/P, 23 cm^2

Legend: conc.: concentration operating mode; D: darkness conditions; Dy: dynamic regime; F$_\sim$: frequential mode; F$_-$: non frequential mode; I$^+$: constant illumination level; I$^-$: flash lamp illumination; n^+: constant ideality factor; n^-: non constant ideality factor; R_s^-: constant series resistance at any illumination level and temperature value; R_{sh}^+: infinite shunt resistance; R_{sh}^-: finite shunt resistance; S: static regime; S-C: single crystal; *: total solar cell area not specified. (*Continued opposite.*)

and both very low intensity and simplified detection mode of the output signal.

(ii) The second, third, fourth, eleventh and twelfth techniques in Table 1 can be considered amongst the simplest and give similar results for our target. Moreover, the first one (under darkness) gives a lower R_s value than values from the previous methods (under illumination, except for the second).

(iii) R_s values obtained by other workers lie in a larger interval: [0; 1600] mΩ cm^{-2}. This disparity is imputable to intrinsic differences amongst methods and to differences in solar cells investigated (disparities in basic materials, structures, fabrication modes and areas). Furthermore, this last difference is the principal origin of the discrepancies often noticed between our results and those of other workers, even for the same methods. Another reason for discrepancies could lie in different experimental conditions used by different workers for the same method.

(iv) Finally, one other general trend remarked from the results of Table 1 is the following: the lower the the solar cell area, the higher the R_s value per unit area. This is evidenced if one compares our results (which correspond to S_t = 78.5 cm^2), with results from refs [13] (S_t = 25.8 cm^2), [21] (S_t = 23 cm^2), [12] (S_t = 4 cm^2) and [7] (S_t = 2 cm^2). This trend is in good agreement with the Lindmayer and Allison relationship [22] which specifies that R_s varies in inverse ratio with the square of the number of front ohmic contact fingers (and this number is proportional to the solar cell area).

6. CONCLUSION

This work of review, test and comparative analysis of different techniques for determination of solar cell series resistance should be useful for further research and development on photovoltaic devices.

Table 1—*continued*

Other parameters invstigated	Other experimental conditions	Number of diodides in the solar cell model	Other assumptions
—	D; S	1	R_s^+; R_{sh}^+; n^+
n	D; Dy; F^-	1	R_s^-; R_{sh}^+; n^-
—	I^+; S	1	R_s^+; R_{sh}^-; n^+
—	I^-; S	1	R_s^+; R_{sh}^-; n^+
—	I^-; F_-	1	R_s^+; R_{sh}^+; n^+
n	I^+; S	1	R_s^+; R_{sh}^-; n^-
I_m; V_m; n	I^+; S	1	R_s^+; R_{sh}^+; n^+
—	I^+; S	1	R_s^+; R_{sh}^+; n^+
—	I^+; S	1	R_s^+; R_{sh}^+; n^+
R_{sh}; n	I^+; S	1; 2; . . .; N	R_s^+; R_{sh}^-; n^-
—	I^+; S	1	R_s^+; R_{sh}^+; n^+
—	I^-; S	2	R_s^+; R_{sh}^+; n^-
—	D; Dy; F_-	1	R_s^-; R_{sh}^+; n^-
—	I^-; F_-	1	R_s^+; R_{sh}^+; n^+
R_{sh}; I_s; I_{ph}	I^+; S	1	R_s^-; R_{sh}^-; n^-
R_{sh}; I_s; n	D; S	1	R_s^+; R_{sh}^-; n^+
—	I	1	R_s^+; R_{sh}^-; n^-
—	I^+; D; S	1	R_s^+; R_{sh}^+; n^+
J_{01}; J_{02}; R_{sh}	D; S	2	R_s^+; R_{sh}^-; n^-
—	I^+; S	1	R_s^+; R_{sh}^-; n^+

Acknowledgements—Our thanks are expressed to ICTP Responsibles (Trieste, Italy) who have enabled our stay in the City of Science, notably for collecting the documents needed for this study.

REFERENCES

1. M. Bashahu and F. Gakwandi, Analyse de quelques paramètres électriques sur deux photopiles au Si de fabrication différente. *Revue Rwandaise sci.*, in press.
2. A. M. Cowley and S. M. Sze, *J. Appl. Phys.* **30**, 3212 (1965).
3. J. Boucher, M. Lescure and J. Vialas, *Proc. EEC Photovoltaic Solar Energy Conf.*, Luxembourg, p. 1044. (27–30 September 1977).
4. D. W. Kammer and M. A. Ludington, Laboratory experiments with silicon solar cells. *Am. J. Phys.* **45**(7), 602–605 (1977).
5. M. Wolf and H. Rauschenbach, Series resistance effects on solar cell measurements. In *Solar Cells*, edited by C. E. Backus, pp. 146–170. IEEE Press (1976).
6. J. A. Cape, J. R. Oliver and R. J. Chaffin, A simplified flashlamp technique for solar cell series resistance measurements. *Solar Cells* **3**, 215–219 (1981).
7. Quanzi Jia and W. A. Anderson, A novel approach for evaluating the series resistance of solar cells. *Solar Cells* **25**, 311–318 (1988).
8. C. M. Singal, Analytical expressions for the series resistance dependent maximum power point and curve factor for solar cells. *Solar Cells* **3**, 163–177 (1981).
9. M. A. Hamdy and R. L. Cell, The effect of the diode ideality factor on the experimental determination of series resistance of solar cells. *Solar Cells* **20**, 119–126 (1987).
10. B. Arcipiani, Generalization of the area method for the determination of the parameters of a non-ideal solar cell. *Rev. Phys. Appl.* **20**, 269–272 (1985).
11. S. K. Agarwal *et al.*, A new method for the measurement of series resistance of solar cells. *J. Phys. D: Appl. Phys.* **14**, 1643–1646 (1981).
12. A. Polman, W. G. J. H. M. Van Sark, W. Sinke and F. W. Saris, A new method for the evaluation of solar cell parameters. *Solar Cells* **17**, 241–251 (1986).
13. J. P. Charles, M. Abdelkrim, Y. M. Muoy and P. Mialhe, A practical method of analysis of the current–voltage characteristics of solar cells. *Solar Cells* **4**, 169–178 (1981).
14. D. Laplaze and I. Youm, Modélisation d'une cellule P. V.: détermination des paramètres à partir de la caractéristique courant–tension à l'obscurité. *Solar Cells* **14**, 179–186 (1985).
15. S. R. Shariwal, S. Mittal and R. K. Mathur, Theory for

voltage dependent series resistance in silicon solar cells. *Solid-State Electron.* **27** (3), 267 (1984).
16. K. Rajkanan and J. Shewchun, A better approach to the evaluation of the series resistance of solar cells. *Solid-State Electron.* **22**, 193 (1979).
17. G. L. Araujo, E. Sanchez and M. Marti, Determination of the two exponential solar cell equation parameters from empirical data. *Solar Cells* **5**, 199–204 (1982).
18. M. S. Imamura and J. I. Portocheller, *Proc. 8th IEEE Photovoltaic Specialists Conf.*, New York, pp. 102–109 (1970).
19. D. K. Bhattacharya, A. Mansigh and P. Swarup, Dependence of series resistance on operating current in *p–n* junction solar cells. *Solar Cells* **18**, 153–162 (1986).
20. H. J. Hovel, *Semiconductors and Semimetals*, Vol. 11: *Solar Cells*. Academic Press, New York (1975).
21. G. L. Araujo *et al.*, *Proc. VIth EEC Photovoltaic Solar Energy Conf.*, London, pp. 138–143 (1985).